PHYSICSAccess Research Paper
ISSN Online: 2756-3898, ISSN Print: 2714-500X https://doi.org/10.47514/phyaccess.2025.5.1.001

Delineating Hot Zone and Lineaments within Vredefort Crater in South Africa through Aeromagnetic Data Inversions

Muhammad B Atif[1], Yongzhi Wang[1, 2], Muhammad P Akhter[3], Bello Y Ayoola[4], Lawal K Muideen[5], Fahad Hameed[6], Kateryna Hlyniana[7], Bo Wen[1], Zubair Nabi[8], Dong Yuhao[1] and Yakubu M Bashir[9]

[1] College of Geoexploration Science & Technology, Jilin University, Changchun 130061, China
[2] Institute of Integrated Information for Mineral Resources Prediction, Jilin University, Changchun 130061, China
[3] National University of Modern Languages Faisalabad Campus, 38100, Pakistan
[4] Department of Physics, Air Force Institute of Technology, Kaduna, Nigeria
[5] Department of Physics, National Open University of Nigeria
[6] Institute of Geology, University of Azad Jammu and Kashmir, Muzaffarabad, Pakistan
[7] School of Mathematics, Jilin University, China
[8]Software Engineering, Government College University Faisalabad, 38000, Pakistan
[9] Department of Physics, Ahmadu Bello University Zaria, Nigeria

Corresponding E-mail: belloya@afit.edu.ng

Received 20-12-2024
Accepted for publication 22-01-2025
Published 24-01-2025

Abstract

The Vredefort Dome has undergone some geologic processes that result in changes in the temperature of the rocks. This study contributes to the discussion on the thermal effect of the impact in the area on a regional scale and also delineates the linear structures around the Dome. The outcome shows that the center of the Dome is characterized by a low Curie point depth (CPD), indicating a high-temperature status that agrees with previous temperature reports in that area. The high-temperature tendency is observed to extend south of the Vredefort dome. The center-south of the Vredefort structure has a high thermal gradient and heat flow. The fractal distribution of the Vredefort structure correlates with the multi-ring structure around the Dome, which is peculiar to a few impact structures on Earth. The trend of the Fractal exponent contour around the center suggests that the contact of the meteoritic body at that region occurs at an angle and then pushes southwards. The structural analysis results show linear structures that are believed to be faults/fractures trending in North-NorthEast (NNE), NorthEast (NE), EastWest (EW), and NorthSouth (NS) directions whose effects have been explained in previous works in the area and were also identified on the ground. Some closures are observed at the center of the multi-ring structure, indicating the melt-dykes around the Vredefort dome. The Euler depth solutions cluster suggests the lineaments are about 7 km deep.

Keywords: Curie point depth; Fractal exponent; Vredefort Dome.

I. INTRODUCTION

The Vredefort Dome in South Africa is among the oldest [1] and the largest [2], [3] of the 190 confirmed impact structures worldwide. The impact crater is caused by the hypervelocity impact of a meteorite involving an instant transfer of kinetic energy in the impacting body. The effect is a geological process involving extreme strain rates and a huge amount of energy, causing an instant increase in the temperature and the pressure producing fracturing, disruption, and structural transformation of the target materials [4], [5], [6].

There are controversies on reports of the temperatures around the center of the Dome and the temperature variation along the radius of the Vredefort Dome [7], [8]. A progressive post-impact increase in temperature in the exterior collar rocks and a local rise in the central core due to the geothermal gradient before impact-induced uplift and shock heating [9]. The center of the Dome was modeled to be of temperature exceeding about 1000 °C [10], [11] and within a 15 km radius of the core was heated above 700 °C [10]. The temperatures of outcrops within an 8 km radius of the central center of the Dome were measured to be within the range of 650 – 700 °C, exceeding the minimum granite solidus [8], [12]. Reference[13] disagreed with the suggestion of [14] that the temperature of the rock in the core did not rise above 500 - 600 °C for 3 min. or 500 °C for 1 hr. The disagreement was due to the report of [10] that modeled the nature of the metamorphism after the impact; after hundreds of thousands of years, the heat from the effect dissipated.

The controversy on the temperatures around the core of the impact structure could be evident in the multiple concentric magnetic patterns, -1400 – 400 nT, without a significant anomaly at the center [15] unlike in other impact structures with negative magnetic anomalies[16]. Tiny single-domain magnetite that was formed under a high pressure (or temperature) environment, which then crystallized along PDFs (planar deformation features), is suggested as the most likely, source of high remanence of magnetism in some drilled samples of the Vredefort structure [17], [18]. The remanence of magnetic particles in PDFs was randomized by a plasma field within a centimeter-scale regime [13], [14], [17]. Apart from the effects of the impact on the local temperatures of rocks resulting in the Curie temperatures of magnetite with the range of 540 – 580 °C [19], [17], [20] and consequently, the nature of the magnetism of the rocks around the core, regional faults (transversely cutting the basement, transcending different geological units and structural orientations) and other structures such as the rim of semicircular ridges and melt dykes were the product of the impact event [15], [21]. Despite controversies about the crater's center temperatures, it still has the hottest temperatures [19]. The discussion on the thermal regime of the dome will be expanded, due to evidence on regional heating near the structure.

This research investigates the regional effect of the impact on the thermal regime and linear structures around the impact structure. For the first time, the Curie point depth (CPD) of the Vredefort structure was computed from the spectral analysis of aeromagnetic data of the study area contributing to the discussion on the impact of the thermal effect in the area on a regional scale and attempt to delineate the potentially high-temperature zone(s) in the area. The Fractal-based approach was used to compute the CPD since magnetic susceptibility, crustal magnetization in particular, and magnetic field show fractal behavior [22], [23], [24]. Due to the reported randomized nature of the magnetic remanence of rocks around the structure's core, the CPD was also computed using the centroid method. The method assumes that magnetic anomalies are characterized by an uncorrelated random distribution of sources [25], [26], [27], [28]. The linear structures were delineated through structural analysis by applying various edge detection methods to the magnetic data. Delineating these structures is essential to map the extent of those that have been reported, which are indicators of geologic transition and signature of thermal and shock effect of the impact event around the crater and discover others that are unknown.

A. Background of the study

The CPD is the point where the magnetism of the magnetite ceases due to the increase in temperature. Ferromagnetic minerals are the dominant carriers of magnetism in rocks. The commonly used Curie temperature of crustal rocks is that of magnetite, 580 °C [29]. At temperatures above this, the ferromagnetic mineral becomes non-magnetic.

The thermal structure of the Earth can be understood from the spatial temperature variation, which can be estimated by calculating the Curie point depth (CPD) from the spectral analysis of magnetic anomaly data [30], [31], [32]. Apart from investigating the thermal structure, CPD helps study global heat loss, which can be achieved by assuming that the lateral compositional variation exerts a negligible influence on the Curie temperature; hence, the Curie point temperature is generally constant in the world [33].

The variation in the Curie-point temperature between regions depends on the nature of the rocks area and the mineral constituents. Hence, shallow Curie point depths are expected to be recorded in areas with a young volcanic regime, geothermal activities, and a thin crust. The region of Curie isotherm can be determined through some spectral magnetic methods based on the flat layer hypothesis, either a random uncorrelated magnetization model or fractal (self-similar) magnetization model [31], [34], [35], [36], [37]. The centroid and fractal-based methods of computing CPD have been thoroughly reviewed [37].

B. Geology of the study area

It is widely accepted that the amphibolite–granulite facies isograd marks the change from middle to lower crustal layers and is a key boundary inside the crust. Fig. 1 shows a cross-section of the amphibolite–granulite facies transition across about 36 km of continental crust [51], [48], [50], [49] exposed

in the Vredefort crater.

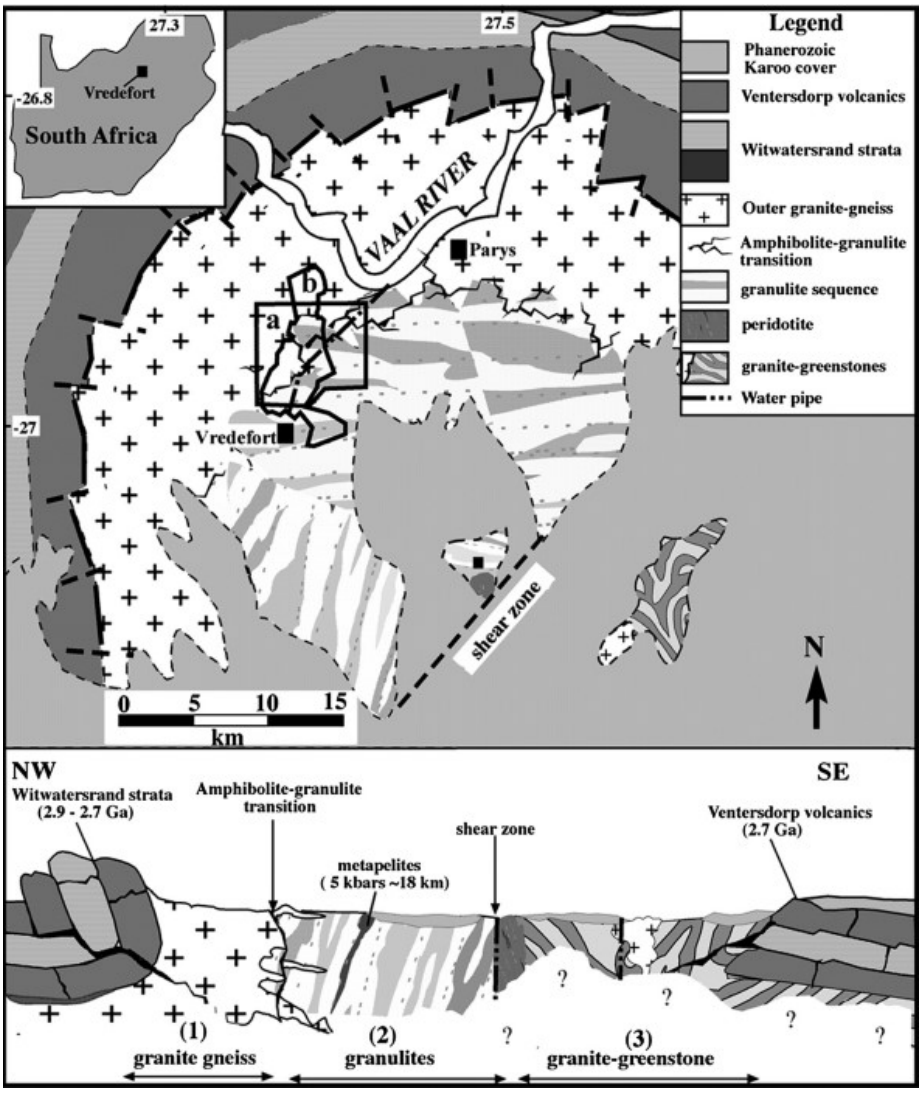

Fig. 1 Geologic map of the Vredefort meteorite impact crater and a northwest-southeast section across it (adapted [49]). Horizontal scale of cross-section same as map; vertical scale exaggerated [15].

The rocks of the granulite facies domain to the south are composed of charnockite and mafic granulite. According to [52] and [53], metapelites in the granulite facies domain, near the transition zone, record peak metamorphic conditions of 800–900 °C and 5–6 kbar, which is consistent with the conclusion that this boundary developed at crustal depths of about 20 km. Underlying the northern map region are the amphibolite facies rocks, which are typically massive to foliated granite-gneiss with coarse grains. The complex mixture of rocks from both domains forms the boundary zone between granite-gneiss and granulite.

The granite-gneiss and charnockitic rocks are intruded by quartz syenites, which usually form elongated bodies that are sub-parallel to the granite-gneiss to granulite border. These bodies range in width from meters to tens of meters. The quartz syenite and granite-gneiss are crosscut by undisturbed impact melt dykes. The basement is traversed by regional impact-related faults contrasting various geological units and structural orientations. Both rock types are dated at approximately 2.0 Ga, and the pseudotachylite breccias originated during the impact event, just as the impact melt dykes [21].

II. MATERIALS AND METHODS

The aeromagnetic data of the Vredefort Dome sourced from https://drive.google.com/drive/folders/0B9In9AOnWyDRRjJYNlhFRWlidkE was used in this study, with the grid of the total magnetic intensity of the area displayed in Fig. 2. Sixteen grids (blocks) with a dimension of about $45 \times 45\ km$ were extracted.

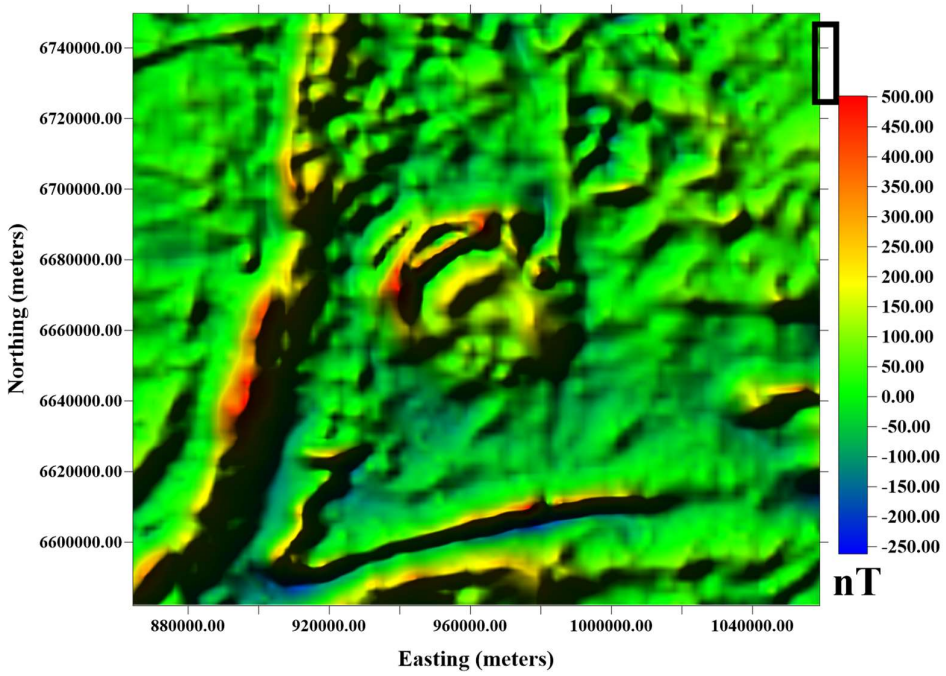

Fig. 2 Total magnetic intensity of the Vredefort structure.

Trend analysis was carried out on each block using the least square polynomial regression approach to yield the residual grid of the study area. Zero-padding and tapering were done on the residual data of each block to take care of the edge effect. The grid of each block was transformed into the frequency domain by performing a Fast Fourier Transform on them. Then the radial average power spectrum was computed, yielding the angular frequency in cyc/km and the natural logarithm of the spectral power of the aeromagnetic data.

The fractal-based approach [37] and the centroid method are used to compute the CPD of the Vredefort Dome. The magnetization of rocks can be affected due to thermal anomalies at depth. Fractals are entities that look similar at a greater variety of scales. Spatial changes in geophysical parameters like density and susceptibility can be described using fractals. Real geologic situations are multifractal [28].

The de-fractal method reduces the ambiguity of fractal parameter selection [37] and provides an estimate of Z_b, which is based on (1).

$$P_F(k_x, k_y) = P_R(k_x, k_y)|2\pi k|^{-\propto} \quad (1)$$

All parameters in the equation have been defined by [37]; wavenumber k, in this case, is in cyc/km. To remove the fractal exponent from the observed power,

$$P_R(k_x, k_y) = P_F(k_x, k_y)|2\pi k|^{\propto} \quad (2)$$

For 2-D bodies, $P_R(k_x, k_y)$ can be written on account of [30] and [38] as in (3).

$$P_F(k_x, k_y) = 4\pi^2 C_m^2 \emptyset_m(k_x, k_y)|\Theta_m|^2|\Theta_f|^2 e^{-2|2\pi k|Z_t}\left(1 - e^{-|2\pi k|(Z_b - Z_t)}\right)^2 \quad (3)$$

The parameters in (3) have been explained by [39].

Re-writing (1) after annular averaging yields (5).

$$P(k) = Ae^{-2|2\pi k|Z_t}\left(1 - e^{-|2\pi k|(Z_b - Z_t)}\right)^2 \quad (4)$$

Determination of Z_t was achieved through (5). The process that led to (5) has been demonstrated by [30], [31], [39], [35].

$$ln(P(k)) = B - 2|2\pi k|Z_t \quad (5)$$

And A can be calculated using (6).

$$A = e^B \quad (6)$$

To compute Z_0, (4) can be transformed to:

$$P(k) = Ce^{-2|2\pi k|Z_0}\left(e^{-|2\pi k|(Z_t - Z_0)} - e^{-|2\pi k|(Z_b - Z_0)}\right)^2 \quad (7)$$

which can be simplified to

$$ln\left(\mathrm{P(k)}^{1/2}/|2\pi k|\right) = D - |2\pi k|Z_0 \quad (8)$$

Reference[35] demonstrated the process to estimate Z_0, and calculating Z_b using (9).

$$Z_b = 2Z_0 - Z_t \quad (9)$$

The flowchart in Fig. 3 demonstrates the step-by-step procedure of the de-fractal approach for determining the fractal parameter and estimating the basal depth.

The geothermal gradient of the heat flow was computed using (10).

$$Thermal\ gradient\ (T) = \frac{580\ ^\circ C}{Z_b} \quad (10)$$

The Curie point of magnetite (580 °C) has been adopted by researchers such as [26] in computing thermal gradient (T). The heat flow (q) of the study area is computed using (11).

$$q = kT \quad (11)$$

Where thermal conductivity (k) of granite, 2.18 $Wm^{-1}k^{-1}$ [40], was adopted to calculate the heat flow of the study area since thermal conductivity is rock-dependent.

A. Structural Analysis

Linear structures are analyzed using edge detection techniques (for the review of the methods, see [41], [42], [43],

[44]. Before applying these techniques, the aeromagnetic data was upward continued up to 1 km to suppress the noise level in the data and enhance the anomalies of interest. Euler deconvolution [45] was implemented to identify the geometry and depths of the linear structures.

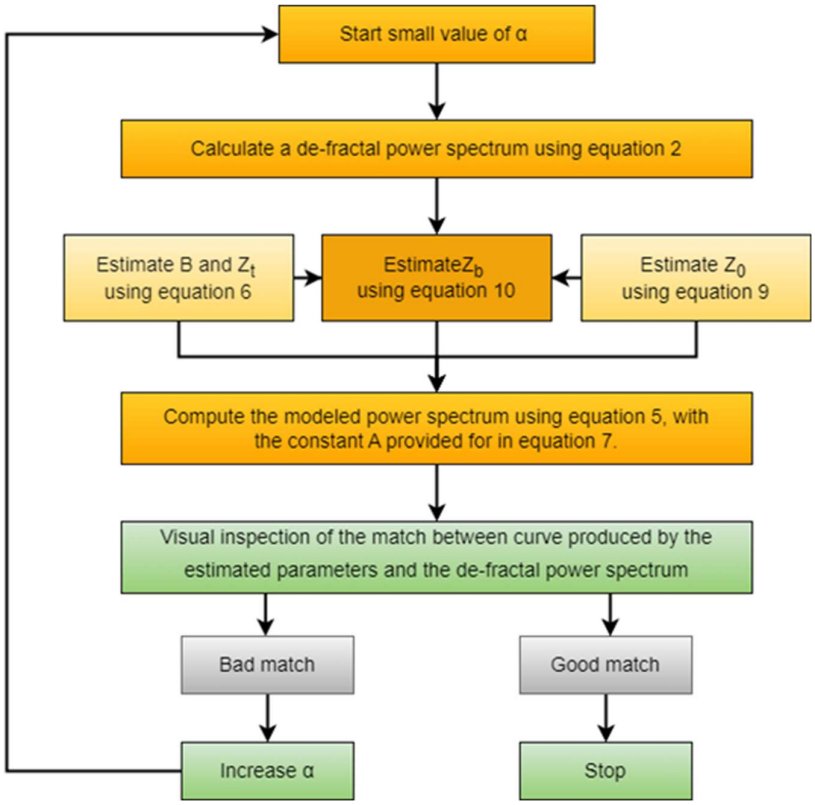

Fig. 3 Flowchart of the de-fractal approach for estimating the depth to the magnetic bottom [37].

III. RESULTS AND DISCUSSION

The center of the Vredefort structure is known to be of high temperature due to the impact of the meteoritic body, which is evident in the high temperatures modeled in rock samples within the core [10] and low aeromagnetic anomalies of about -1400 nT [15] but little is known of the temperature variation of the entire structure. The computation of the CPD of the whole structure will provide a good perspective of the temperature distribution of the Vredefort structure.

The Defractal approach was implemented on the power spectrum of the fast Fourier-transformed residual data of block 1. The application of the technique needs no prior knowledge of the fractal parameter. Firstly, the α value of 0.5 was used to calculate the de-fractal spectrum of the aeromagnetic data of block 1. Depths to the top, centroid, and bottom, and the constant, B, were estimated from the de-fractal data. All the necessary parameters were then used to compute the model power spectrum. The de-fractal power spectrum, modeled power spectrum, and observed power spectrum were plotted together to observe the match between modeled and de-fractal power spectrum (Fig. 4a). The fit between the modeled and de-fractal power spectrum gradually improves as the fractal exponent increases to 0.9 (Fig. 4b). A good fit was obtained at α = 1 (see Fig. 4c).

The visual fit assessment was done, considering all the main features with special attention at the low wavenumber region as it constitutes a region of the deep-seated body. To guarantee possible solutions at higher α are not missed, a fractal value of α = 1.2, 1.8, 2, 2.1, 3, 4 was used (see Fig. 4d - i). The fractal exponents and Curie depth that yield a good fit in each block are listed in Table I, and the contour map of the calculated Curie depth based on the fractal approach is presented in Fig. 5a. The Curie depth ranges from 1.1 to 12.5 km and an average value of 4.4 km. The center of the structure has a shallow CPD of about 2 km, which implies a high Curie temperature, and it agrees with the previous report about the center of the Dome as having the hottest temperatures [13], [14], [8], [10], [11], [12], [7], [19]. The shallow depth observed at the core of the Dome decreases south of the center; this could explain the origin of the negative aeromagnetic anomalies around the enigmatic crater [15].

The centroid method which assumes that the magnetic anomaly source is a function of uncorrelated random magnetization, was used to compute the CPD of the entire structure. The Z_t and Z_o of the magnetic field in block 1 were

estimated as shown in the spectral plot in Fig. 4, and then the Curie depth was calculated using the estimated depths.

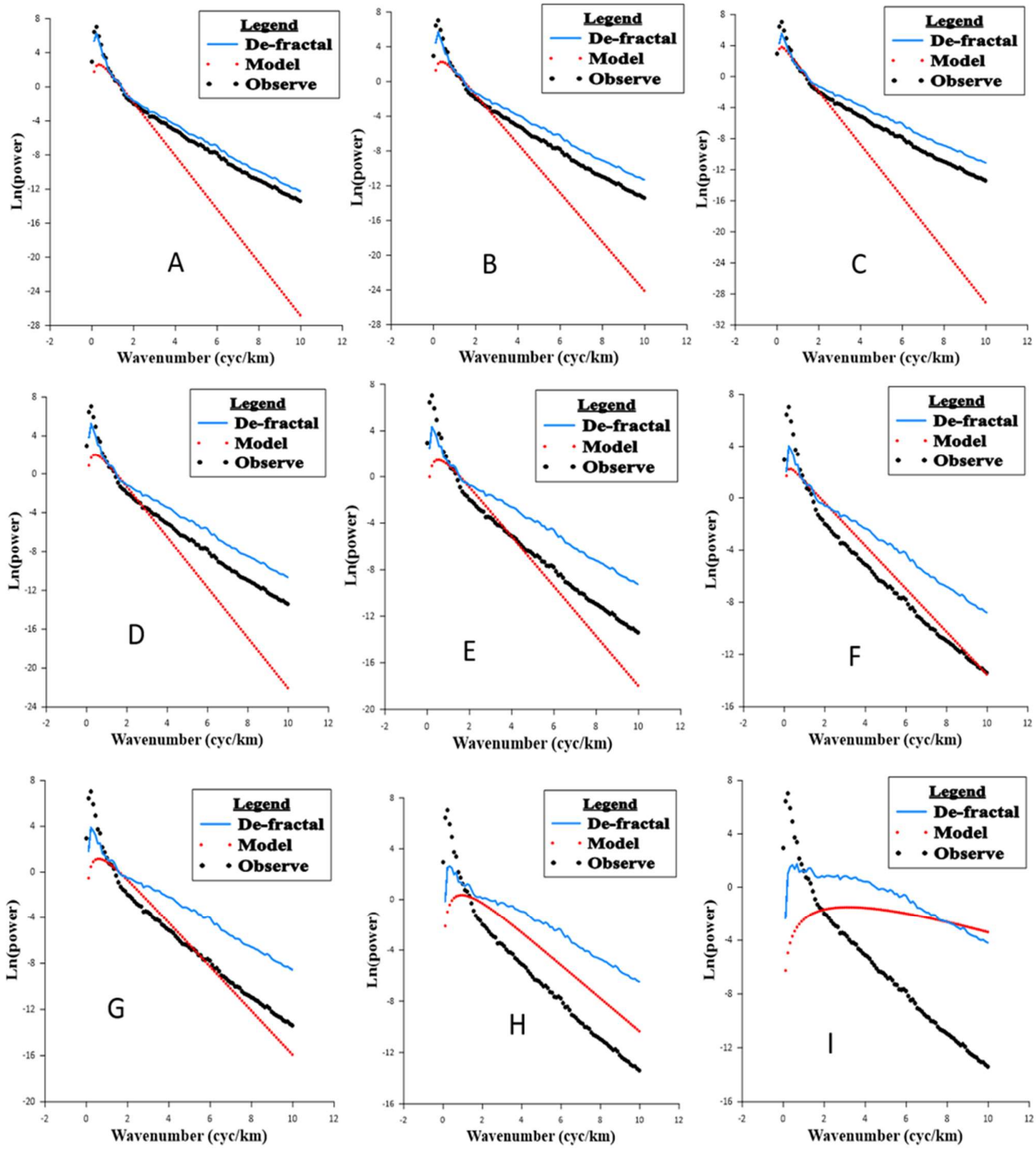

Fig. 4 Spectral plot at each fractal exponent.

The calculated Curie depths of the entire area (see Table I) were subsequently used to produce the CPD contour map of the Vredefort structure (Fig. 6). The Curie of the area ranges from 5.9 to 15 km with an average depth of 10.7 km. The high CPD of about 10.5 km observed at the center of the structure (Fig. 5b) disagrees with the high temperature reported about the area. This result also affirms the argument of [15] on the report of [20]. The shallow result of Curie depth based on the Centroid approach at the southern and eastern edges of the study area suggests high temperatures in those regions. In contrast, the deep Curie depth result in the northern and western regions suggests low temperatures.

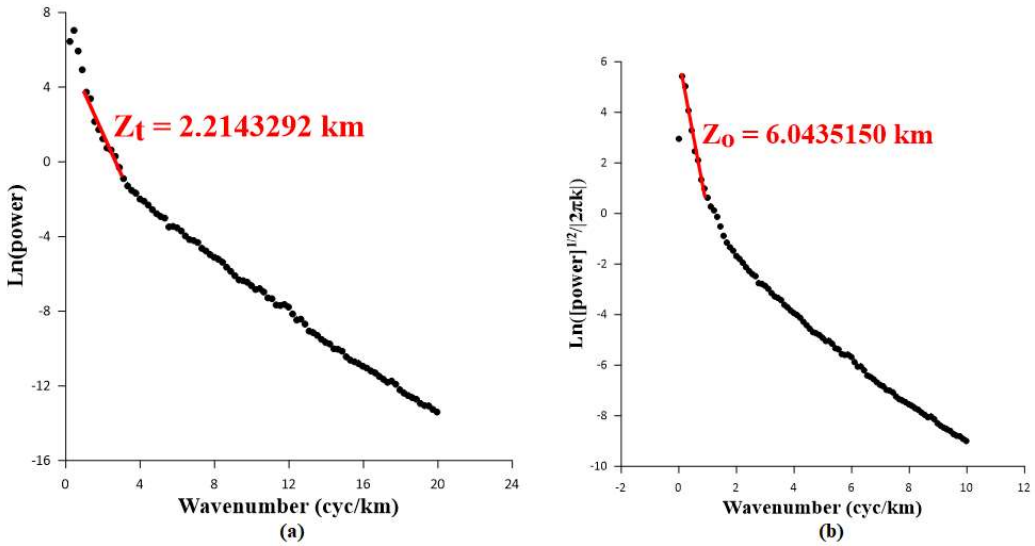

Fig. 5 Spectral plot to estimate (a) Zt and (b) Zo

Table I. Depth parameters determined from the methods.

Block	A	De-fractal method Zb	Centroid method Zb
1	1	7.9403231	9.8727008
2	2.8	1.124313	6.9943294
3	1.5	1.5054757	5.9336695
4	-1	4.4378556	10.7989829
5	1.5	12.4583024	14.4571468
6	3.5	1.1390114	13.3349918
7	2	2.8856921	10.5401224
8	1	3.7282553	9.9402322
9	0.5	4.2939627	11.3721624
10	0.5	3.9496275	11.4824229
11	0.5	2.972995	11.6701282
12	0.2	2.92835	7.2971815
13	-1	5.9316429	11.5710796
14	0.1	6.5745297	15.0319729
15	-0.5	4.0928435	9.8295267
16	-0.5	4.2814734	11.1554817

As a result of the deviation of the Curie depth result of the Centroid-based approach from the known temperature situation at the center of the crater, the Curie depth based on the De-fractal method is thus used to calculate the area's thermal gradient and heat flow. The calculated thermal gradient of the structure ranges between 20 and 500 °C/km, and the structure's center recorded a gradient of about 500 °C/km (Fig. 6a). The calculated heat flow ranges between 50000 and 550000 mW/m^2, and the center recorded a heat flow of about 550000 mW/m^2 (see Fig. 6b).

Fractal distribution usually correlates with the geology [46], [47]. The Vredefort crater is among the few multi-ring craters known on Earth [15]. The pattern of the fractal distribution of the Vredefort (Fig. 7a) reveals multiple ring structures around the Vredefort crater. It correlates with the semicircular pattern of the geology of the crater (Fig. 7b). The trend around the structure's core suggests that the impact occurs at an angular position, pushing the impacted body southwards.

The melt-dykes, faults, and other linear structures are evidence of the thermal and shock effects accompanying the meteoritic impact event at Vredefort. NNE linear feature that is prominent for having negative anomaly and of an average amplitude of about 1500 nT, and an NW trending lineament characterized by a change in magnetic field strength which roughly follows the transition zone of the geologic units cut across the entire central part of the crater. The NW trending lineament correlates with the NW trending fault [15]. Structural analysis through total horizontal derivatives is essential to delineate linear structures, which are the manifestation of faults, fractures, and dykes in the study area. The known NNE and NW trending at the crater's center appear as part of the multi-ring structure characterized by the high amplitude of the total horizontal magnetic gradient tapering towards the south. Some closures are observed at the center of the multi-ring structure, which could indicate intrusive. East-North-East (ENE) trending lineaments are prominent in the south of the study area. An NS trending feature extends from the north, passing through the eastern edge of the multi-ring structure at the center and cross-cutting the ENE linear structures south of the study area. NNE trending lineaments extending from the north to the southwestern end of the study area were also observed (see Fig. 8). The linear structures (Fig. 9a) are believed to be manifestations of faults.

It is assumed that negative magnetic anomaly is caused by the uniformly magnetized body of intrusive melt rock that was emplaced at a depth of 1 – 7 km at the subsurface at the time of the impact [48]. The only good reason for this is the evidence of ~2 Ga intrusive rocks in the form of impact melt dykes and pseudotachylite [15]. The Euler depth solutions of dyke at the center of the crater where melt- dykes have been

identified on the ground show a depth result of 1.5 – 7 km (Fig. 9b). The NNE trending structure which forms a multi-ring structure at the center, has a depth solution of ~100 m. The shallow depth solution could explain the negative anomaly reported along its path. The NS trending passing from north to south is expected to be exposed at the north end and close to the middle of the study area as the dyke solutions around the region are <100 m deep. The NNE trending lineament appears deep up to 7 km but is expected to be exposed at the northern end of the study area.

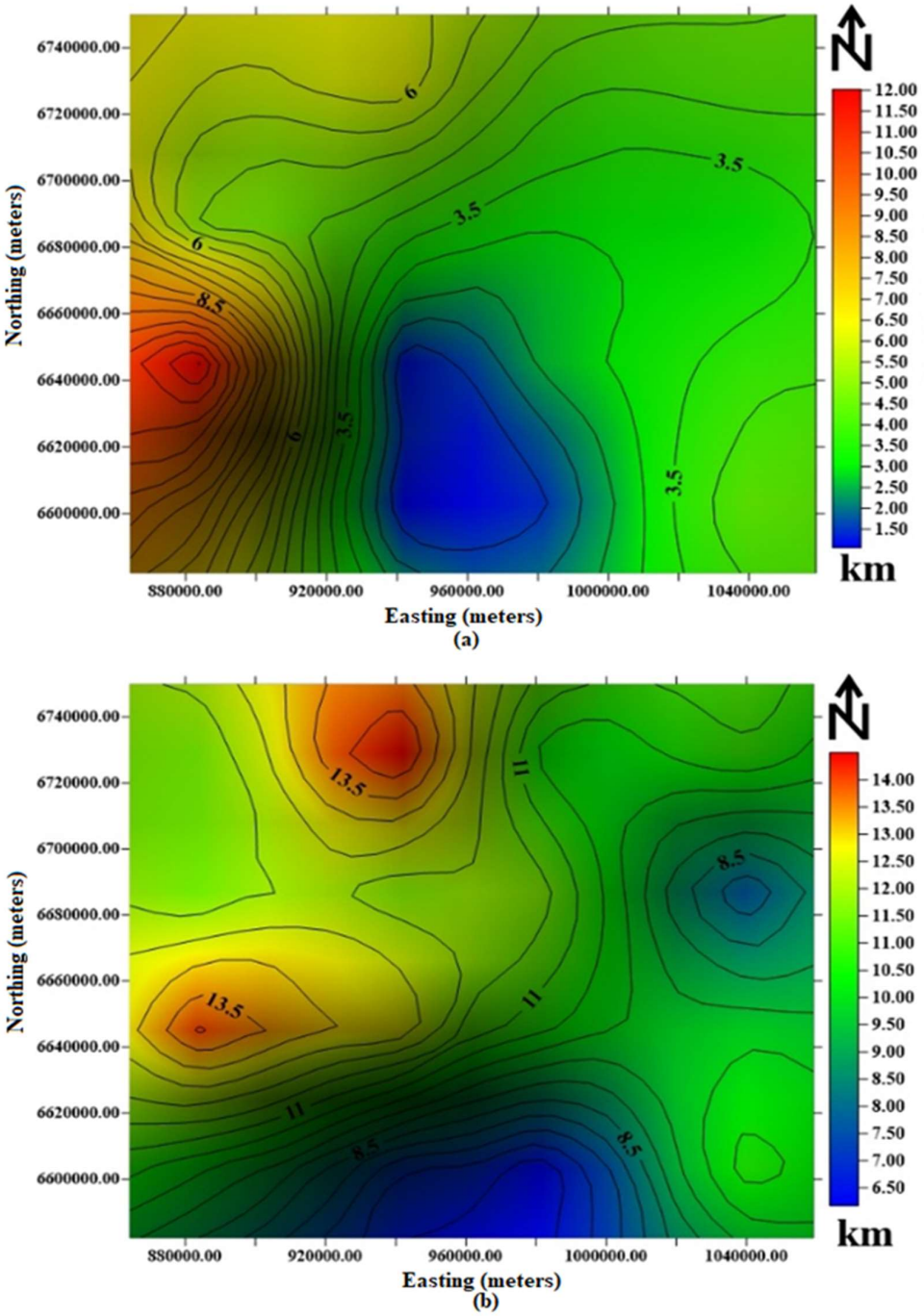

Fig. 6 Curie point depth of the Vredefort structure using (a) Fractal-based method (b) Centroid-based method.

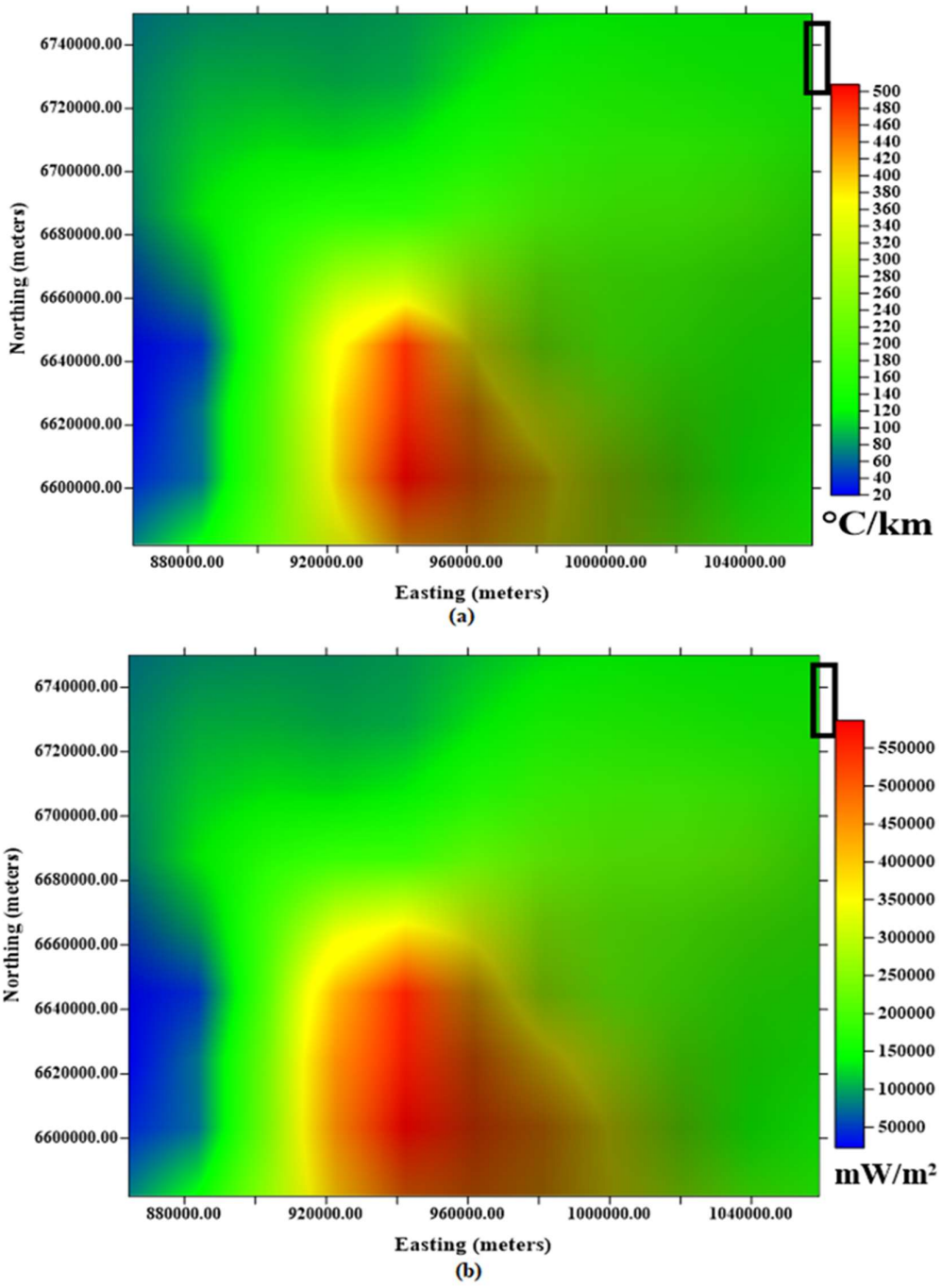

Fig. 7 (a)The geothermal gradient map (b) the heat-flow map of the Vredefort structure.

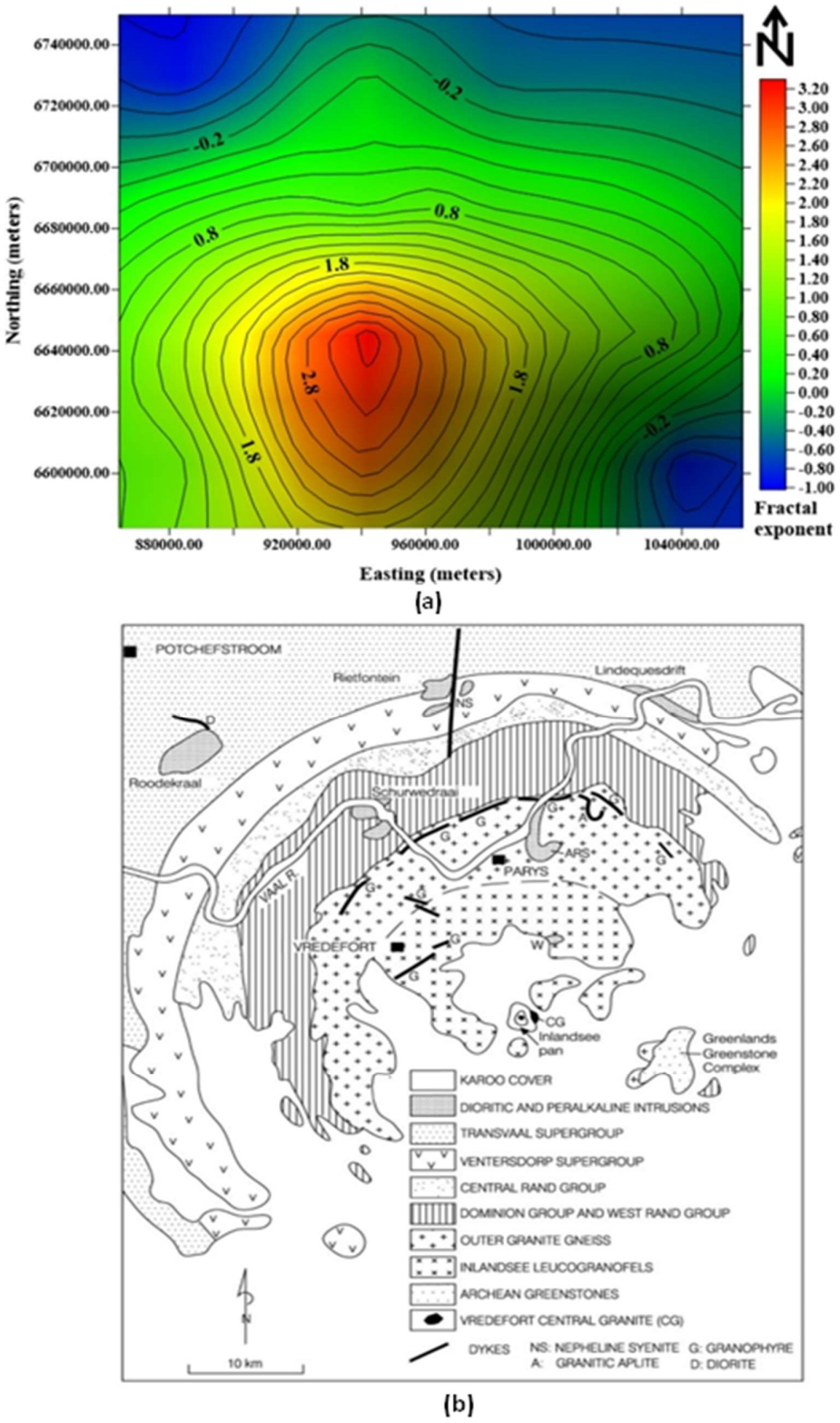

Fig. 8 (a)The fractal exponent distribution within the study area. (b) simplified geology map of the core of Vredefort structure [8].

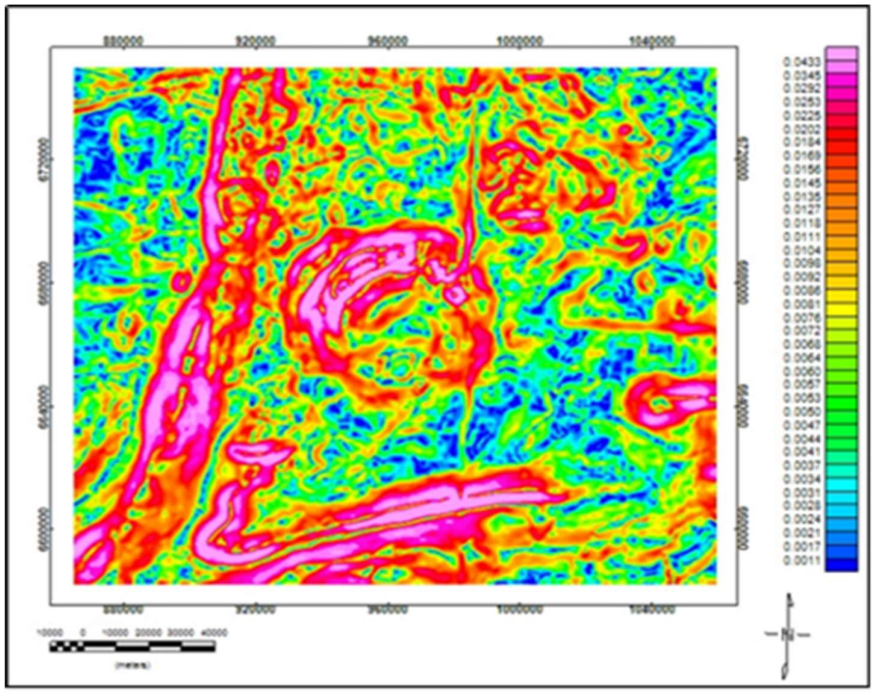

(a)

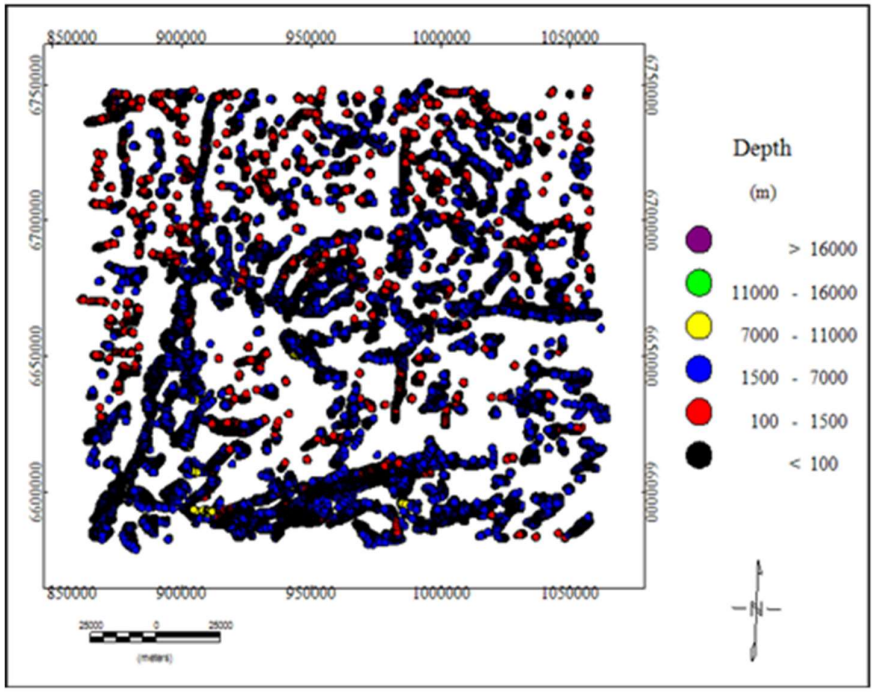

(b)

Fig. 9 (a)Total horizontal derivative map of the Vredefort structure. (b) Euler depth solution of dykes within the Vredefort structure.

The depth parameters determined from the De-fractal and Centroid methods are shown in Table I. The De-fractal method uses the value of α as the fractal exponent, which controls the scaling behavior of the setting. The α value affects the spatial distribution of the depth parameters, allowing the characterization of the subsoil layer to be described. For

example, in block 1, the De-fractal method gives a depth parameter (Zb) of 7.9403231, which indicates the estimated depth of underground structures. On the other hand, the Centroid method does not require α values and provides depth parameter values without relying on fractal analysis. In block 1, the Centroid method calculates a depth parameter of 9.8727008, suggesting a different view of the subsurface structure. Comparing the results of the two methods shows that the depth parameters show variation in the study area. The range of depth parameter values obtained from the De-fractal method extends from 1.124313 to 12.4583024, while the Centroid method gives the range from 5.9336695 to 15.0319729.

These variations reveal subsurface structural and compositional heterogeneity in the Vredefort Dome region. To fully understand the implications of these depth parameters, it is important to consider the geological context and the specific objectives of the study. Interpreting these values may involve correlating them with known geological features, such as fault systems or lithological boundaries, to understand subsurface architecture better. In addition, comparisons with previous studies or theoretical models can help confirm and refine the results. The depth parameters obtained from both methods contribute to a better understanding of depth variation in the study area. They may guide future investigations of the Vredefort Dome area, elucidating its history, geological history, and potential geological resources.

IV. Conclusion

This study provides an update to the discussion on the temperature of the Vredefort structure through the computation of the Curie point depth. Shallow CPD is observed at the center of the structure, indicating high-temperature status, which agrees with previous temperature reports in that area. The high-temperature tendency is observed to extend south of the Vredefort dome. A high thermal gradient and heat flow also characterize the Vredefort structure's center-south. It is recommended that the temperature of outcrops at the shallow Curie point depth region south of the study be investigated. The fractal distribution of the Vredefort structure correlates with the multi-ring structure around the Dome, which is peculiar to few impact structures on Earth. The trend of the Fractal exponent contour around the center suggests that the contact of the meteoritic body at that region occurs at an angle and then pushes southwards.

The structural analysis results show linear structures that are believed to be faults/fractures trending in NNE, NE, EW, and NS directions whose impacts are explained in previous works in the area and were also identified on the ground. It also delineates the melt-dyke around the Vredefort dome. The Euler depth solutions cluster around the study area's linear structures, suggesting they are about 7 km deep. The linear structures delineated are recommended to be identified on the ground to understand their morphology further.

CONFLICT OF INTEREST

The authors declare that they have no known competing financial or other interests that could have influenced this study.

DATA AVAILABILITY

Data analyzed are available on demand in the Google repository.https://drive.google.com/drive/folders/0B9In9AOnWyDRRjJYNlhFRWlidkE.

References

[1] H. Henkel, and W. U. Reimold. “Integrated geophysical modelling of a giant, complex impact structure: anatomy of the Vredefort Structure, South Africa”. Tectonophy., vol. 287, pp. 1 – 20, 1998.

[2] R. L. Gibson and W. U. Reimold. “The Vredefort impact structure: South Africa (the scientific evidence and a two-day excursion guide)”. Memoir 92, Council for Geosci., Pret., pp. 110, 2001.

[3] R .L. Gibson and W. U. Reimold. “Geology of the Vredefort impact structure: a guide to sites of interest”. Memoir 97, Council for Geosci., Pret., pp. 182, 2008.

[4] C. Koeberl. “Identification of meteoritic components in impactites. In: Grady, M. M., Hutchison, R., McCall, G. J. H. and Rothery, D. A. (eds) Meteorites: Flux with Time and Impact Effects”. Geol. Soc., Lond., Spec. Pub., 140; 133 – 153, 1998.

[5] C. Koeberl. “The Geochemistry and Cosmochemistry of Impacts. In: Treatise on Geochemistry” 2007.

[6] S. D. Montalvo, A. J. Cavosie, T. M. Erickson, and C. Talavera. “Fluvial transport of impact evidence from cratonic interior to passive margin: Vredefort-derived shocked zircon on the Atlantic coast of South Africa”. Amer. Mineralogist, vol. 102, pp. 813 – 823, 2017.

[7] R. L. Gibson, R. L. Armstrong and W. U. Reimold. “The age and thermal evolution of the Vredefort impact structure: a single-grain U–Pb zircon study”. Geochim. Cosmochim. Acta, vol. 61, pp. 1531 – 1540, 1997.

[8] R. L. Gibson, and W. U. Reimold. “Shock pressure distribution in the Vredefort impact structure, South Africa”. Geol. Soc. Amer., Spec. Paper, vol. 384, pp. 329 – 349, 2005.

[9] C. Lana, R. L. Gibson, and W. U. Reimold. “Impact tectonics in the core of the Vredefort Dome, South Africa: Implications for central uplift formation in very large impact structures”. Meteoritics & Planetary Sci., vol. 38, pp. 1093 – 1107, 2003.

[10] B. A. Ivanov. "Numerical modeling of the largest terrestrial meteorite craters". Solar Sys. Res., vol. 39, no. 5, pp. 381 – 409, 2005.
[11] E. P. Turtle, E. Pierazzo, and D. P. O'Brien. "Numerical modeling of impact heating and cooling of the Vredefort impact structure". Meteoritics & Planetary Sci., vol. 38, pp. 293 – 303, 2003.
[12] R. L. Gibson. "Impact-induced melting of Archean granulites in the Vredefort Dome, South Africa. I. Anatexis of metapelitic granulites". J. of Meteoritic Geol., vol. 20, pp. 57 – 70, 2002.
[13] J. Salminen, L .J. Pesonen, W. U. Reimold, F. Donadini and R. L. Gibson. "Paleomagnetic and rock magnetic study of the Vredefort impact structure and the Johannesburg Dome, Kaapvaal Craton, South Africa—Implications for the apparent polar wander path of the Kaapvaal Craton during the Mesoproterozoic". Precambrian Res., vol. 168, pp. 167 – 184, 2009. doi:10.1016/j.precamres.2008.09.005
[14] L. Carporzen, S. A. Gilder and R. J. Hart. "Origin and implications of Verwey transitions in the basement rocks of the Vredefort meteorite crater, South Africa. Earth & Planetary Sci. Lett., vol. 251, pp. 305 – 317, 2006.
[15] M. Muundjua, R. J. Hart, S. A. Gilder, L. Carporzen, and A. Galdeano. "Magnetic imaging of the Vredefort impact crater, South Africa". Earth & Planetary Sci. Lett., vol. 261, pp. 456 – 468, 2007.
[16] K. Kiik, J. Plado, M. Lingadevaru, S. H. Jeelani and M. Szyszka. "Magnetic Anomaly and Model of the Lonar Meteorite Impact Crater in Maharashtra, India". Geosci., vol. 10, pp. 417 – 430, 2020. doi;10.3390/geosciences10100417
[17] R. J. Hart, S. H. Connell, M. Cloete and L. Mare. "'Super magnetic' rocks generated by shock metamorphism from the centre of the Vredefort impact structure, South Africa". South African J. of Geol., vol. 103, pp. 151 – 155, 2000.
[18] M. Cloete, R. J. Hart, H. K. Schmid, M. Drury, C. M. Demanet and K. V. Sankar. "Characterization of magnetite particles in shocked quartz by means of electron- and magnetic force microscopy: Vredefort, South Africa". Cont. to Mineralogy & Petrology, vol. 137, pp. 232 – 245, 1999.
[19] R. J. Hart, R. B. Hargraves, M. A. G. Andreoli, M. Tredoux, Doucouré. "Magnetic anomaly near the center of the Vredefort structure: implications for impact related magnetic signatures". Geol., vol. 23, pp. 277 – 280, 1995.
[20] L. Carporzen, S. A. Gilder, and R. J. Hart. "Palaeomagnetism of the Vredefort meteorite crater and implications for craters on Mars". Nature, vol. 435, pp. 198 – 201, 2005.
[21] R. M. Flowers, D. F. Moser and R. J. Hart. "Evolution of the amphibolite–granulite facies transition exposed by the Vredefort impact structure, Kaapvaal Craton", South African J. of Geol., vol. 111, pp. 455 – 470, 2003.
[22] V. P. Dimri, and S. S. Ganguli. "Fractal theory and its implication for acquisition, processing and interpretation (API) of geophysical investigation: a review". J. of Geol. Soc. India, vol. 93, no. 2, pp. 142 – 152, 2019. https://doi.org/101007/-s12594-019-1142-8.
[23] M. Fedi. "Global and local multiscale analysis of magnetic susceptibility data". Pure App. Geophy., vol. 160, no. 12, pp. 2399 – 2417, 2003.
[24] M. Pilkington, M .E. Gregotski and J. P. Todoeschuck. "Using fractal crustal magnetization models in magnetic intrpretation". Geophysical Prospecting, vol. 42, no. 6, pp. 677 – 692, 1994. https://doi.org/10.1111/j.1365-2478.1994.tb00235.x
[25] W. Quintero, O. Campos-Enriquez, and O. Harnandez. "Curie point depth, thermal gradient, and heat flow in the Colombian Caribbean (northwestern South America)". Geothermal Energy, Springer 7; 16, 2019. https://doi.org/10.1186/s40517-019-0132-9.
[26] E. M. Abraham, E. G. Obande, M. Chukwu, C. G. Chukwu and M. R. Onwe. "Estimating depth to the bottom of magnetic sources at Wikki Warm Spring region, northeastern Nigeria, using fractal distribution of sources approach". Turk. J. of Earth Sci., vol. 24, 2015. doi:10.3906/yer-1407-12
[27] Bansal, G. Gabriel, V. Dimri. "Power law distribution of susceptibility and density and its relation to seismic properties: an example from the German Continental Deep Drilling Program (KTB)". J. of App. Geophy., vol. 72, no. 2, pp. 123 – 128, 2010. https://doi.org/10.1016/j.jappgeo.2010.08.001.
[28] A. R. Bansal, G. Gabriel, V. P. Dimri and C. M. Krawczyk. "Estimation of depth to the bottom of magnetic sources by a modified centroid method for fractal distribution of sources: An application to aeromagnetic data in Germany". Geophy., vol. 76, no. 3, 2011. https://doi.org/10.1190/1.3560017.
[29] H. E. Ross, R. J. Blakely and M. D. Zoback. "Testing the use of aeromagnetic data for the determination of Curie depth in California". Geophy., vol. 71, no. 5, 2006. https://doi.org/10.1190/1.2335572.
[30] A. Spector and S. Grant. "Statistical models for interpreting aeromagnetic data". Geophy., vol. 35, pp. 293 – 302, 1970.
[31] B. K. Bhattacharyya and L. K. Leu. "Analysis of magnetic anomalies over Yellowstone National Park: Mapping of Curie point isothermal surface for geothermal reconnaissance". J. of Geophy. Res., vol. 80, no. 32, pp. 4461 – 4465, 1975. https://doi.org/10.1029/jb080i032p04461.
[32] F. Bilim, T. Akay, A. Aydemir and S. Kosaroglu. "Curie point depth, heat-flow and radiogenic heat production deduced from the spectral analysis of the aeromagnetic data for geothermal investigation on

the Menderes Massif and the Aegean Region, western Turkey". Geothermics, vol. 60, pp. 44 – 57, 2016. https://doi.org/10.1016/j.geothermics.2015.12.002.

[33] C. F. Li, Y. Lu and J. Wang. "A global reference model of Curie-point depths based on EMAG2". Sci. Rep., 2017. https://doi.org/10.1038/srep4 5129.

[34] S. Maus, D. Gordon and D. J. Fairhead. "Curie temperature depth estimation using a self-similar magnetization model". Geophy. J. Int., vol. 129, pp. 163 – 168, 1997.

[35] A. Tanaka, Y. Okubo and O. Matsubayashi. "Curie point depth based on spectrum analysis of the magnetic anomaly data in East and Southeast Asia". Tectonophy., vol. 306, no. 3 – 4, pp. 461 – 470, 1999. https://doi.org/10.1016/S0040-1951(99)00072-4.

[36] C. Bouligand, J. M. G. Glen and R. J. Blakely. "Mapping Curie temperature depth in the western United States with fractal model for crustal magnetization". J. of Geophy. Res., vol. 114, 2009. doi:10.1029/2009JB006494.

[37] A. Salem, C. Green, D. Ravat, K. H. Singh, P. East, J. D. Fairhead, S. Mogren and E. Biegert. "Depth to Curie temperature across the central Red Sea from magnetic data using the de-fractal method". Technophy., vol. 624–625, pp. 75 – 86, 2014. https://doi.org/10.1016/j.tecto.2014.04.027.

[38] R. J. Blakely. "Potential Theory in Gravity and Magnetic Applications". Cambridge University Press, Cambridge. U.K., 1995.

[39] Y. Okubo, R. J. Grant, R. O. Hansen, K. Ogawa and H. Tsu. "Curie point depths of the Island of Kyushu and surrounding areas, Japan". Geophy., vol. 53, no. 3, pp. 481 – 494, 1985.

[40] J. Kim, Y. Lee and M. Koo. "Thermal properties of granite from Korea". AGU Fall Meeting 2007, abstract #T11B-0576

[41] S. Zhou, D. Huang and J. Jiao. "Total horizontal derivatives of potential field three-dimensional structure tensor and their application to detect source edges". Acta Geodaetica et Geophysica, vol. 52, pp. 317 – 329, 2017. DOI:10.1007/s40328-016-0171-7.

[42] I. M. Ibraheem, M. Haggag and B. Tezkan. "Edge Detectors as Structural Imaging Tools Using Aeromagnetic Data: A Case Study of Sohag Area, Egypt". Geosci., vol. 9, pp. 211 – 224, 2019. doi:10.3390/geosciences9050211

[43] G. Ma, X. Du, L. Li and L. Meng. "Interpretation of magnetic anomalies by horizontal and vertical derivatives of the analytic signal". App. Geophy., vol. 9, no. 4, pp. 468 – 474, 2012. DOI:10.1007/s11770-012-0350-4

[44] W. Wang, G. Zhang and J. Liang. "Spatial variation law of vertical derivative zero points for potential field data". App. Geophy., vol. 7, no. 3, pp. 197 – 209, 2010. DOI:10.1007/s11770-010-0255-z

[45] Q. Pan, D. Liu, S. Feng, M. Feng and H. Fang. "Euler deconvolution of the analytic signals of the gravity gradient tensor for the horizontal pipeline of finite length by horizontal cylinder calculation". J. of Geophy. & Eng., vol. 14, pp. 316 – 330, 2017.

[46] K. M. Lawal, M. N. Umego and S. B. Ojo. "Geological mapping using fractal technique". Nig. J. of Phy., vol. 18, no. 2, pp. 277 – 286, 2005.

[47] K. M. Lawal, M. N. Umego and S. B. Ojo. "New insight into Geology of the Chad Basin". Nig. J. of Phy., vol. 17S, pp. 165 – 169, 2005.

[48] R. J. Hart, M. A. G. Andreoli, M. Tredoux and M. J. de Wit. "Geochemistry across an exposed section of Archean crust at Vredefort: with implications for mid-crustal discontinuities". Chem. Geol., vol. 82, pp. 21 – 50, 1990.

[49] R. J. Hart, I. McDonald, M. Tredoux, M. J. de Wit, R. W. Carlson, M. A. G. Andreoli and L. D. Ashwal. "New PGE and Re/Os-isotope data from lower crustal sections of the Vredefort Dome and a reinterpretation of its "crust on edge" profile. In: de Wit, M.J., Richardson, S.H., Ashwal, L.D. (Eds.), Kaapvaal Craton — Special Publications", S. A. J. Geol., vol. 107, pp. 83 – 94, 2004.

[50] D. E. Moser, R. J. Hart and R. M. Flowers. "Birth of the Kaapvaal tectosphere 3.08 billion years ago". Sci. 291, pp. 465 – 468, 2001.

[51] W. F. Slawson, "Vredefort core: a cross section of the upper crust?" Geochim. Cosmochim. Acta, vol. 40, pp. 117 – 121, 1976. https://doi.org/10.1016/0016-7037(76)90199-X.

[52] W. Schreyer. "Metamorphism and fluid inclusions in the basement of the Vredefort dome, South Africa: guidelines to the origin of the structure". J. Petrol. 24: 26 – 47, 1983.

[53] G. Stevens, R. L. Gibson and G. T. R. Droop. "Mid-crustal granulite facies metamorphism in the central Kaapvaal craton: the Bushveld complex connection". Precambrian Res., vol. 82, pp. 113 – 132, 1997.